J. Fluid Mech. (1970), *vol.* 40, *part* 2, *pp.* 423–432
Printed in Great Britain

Jet noise simulation on shallow water

By R. B. WEBSTER
Department of Aeronautics, Imperial College, London, S.W. 7

(Received 29 July 1969)

A quantitative shallow water simulation technique for aerodynamic noise study is investigated. The technique is employed for the case of a free jet issuing from a nozzle with variable wall roughness.

The experimental results obtained are in remarkably good agreement with the theory. It is concluded that there is great potential for further work in even less well understood areas of aerodynamic noise research.

Introduction

Surface waves on a shallow layer of water are easily visualized and their velocity of propagation is low enough for their origin and development to be followed. The propagation of these waves is, in general, dispersive. At one particular depth ($h = 0{\cdot}48$ cm) however, all but the shortest wavelengths become virtually non-dispersive and thus provides a basis for sound simulation. This method of simulation appears promising, particularly so in the study of problems which are not well understood. Jet noise is just such a problem.

Ffowcs Williams & Hawkins (1968) have shown that surface waves on a shallow layer of water and aerial waves originating from turbulence are generated by a similar distribution of quadrupoles and surface dipoles. They developed a shallow water theory for a turbulent free jet considering the radiation field to arise from eddies convected along the jet. The eddies radiate as quadrupoles in precisely the same manner as the aerodynamic case. The parametric behaviour of the radiation in the far field is the same as that for the two-dimensional aerial case. This is a seventh power velocity law with a Doppler factor modified to take the eddy lifetime into account.

The theory is based on the assumption that the radiation is purely a by-product of the turbulence. It is also assumed that both the jet geometry and the turbulence length scale are independent of jet speed and that the turbulence length scale is set by the jet width. The turbulence is assumed to arise and be maintained by the instability of the jet and to be independent of turbulence already present due to nozzle effects. The eddies thus created have a lifetime assumed to depend only on l/u where l is the eddy length scale and u the eddy velocity.

The turbulence associated with the nozzle makes an additional contribution to the radiation field. Two sources due to the nozzle are present. Turbulence especially on the inlet side of the nozzle causes fluctuations in the mass flow rate through the nozzle, thus producing monopole radiation from the nozzle

exit. Turbulence emerging from the nozzle produces localized fluctuations in mass flow rate in the exit plane which at any instant add to zero over the whole of the nozzle exit. This produces a dipole source for radiation wavelengths longer than the dipole length scale (set by the nozzle width) and a monopole source for shorter wavelengths. The transition from one mode to the other essentially occurs at the sonic speed.

By incorporating all these effects, we obtain the parametric dependence of the radiation intensity (mean square wave amplitude) in the far field to be

$$\overline{(h-h_0)^2} \sim M^7[(1-M\cos\theta)^2+b^2M^2]^{-2}+BM^5+AM^3 \quad (M<1), \tag{1}$$

$$\overline{(h-h_0)^2} \sim M^7[(1-M\cos\theta)^2+b^2M^2]^{-2}+(B+A)M^3 \quad (M>1), \tag{2}$$

where M is the convection Mach number (actually it is the Froude number, but for the sake of analogy it will be referred to as the Mach number); θ is the radiation direction measured from the jet stream to the observation position; b is a small numerical factor determined by the eddy lifetime, B is a factor determined by the relative strength of the nozzle exit turbulence source and A the relative strength of the fluctuating mass flow rate source.

Experimentally the variation of B with nozzle roughness was easily investigated, since the exit plane turbulence was largely independent of inlet turbulence. Reynolds number scaling was not attempted in these experiments but this was not considered a weakness on the grounds that if fully developed turbulence can be maintained in the jet then the radiation field should be relatively insensitive to Reynolds number. This is certainly true in the aerodynamic case, though the Reynolds numbers are usually much greater than those in the present case. The Reynolds numbers here range from about 2,500 to 40,000 based on the nozzle width.

A 2·5 cm nozzle with variable wall roughness was used to provide the jet. The field intensity was measured for various jet speeds at a point in the far field. A capacitance proximity gauge was used as the wave monitoring transducer.

Data gathering was complicated by the difficulty of maintaining the correct ambient water depth steadily for the sampling period. A rate of about three data points per hour was achieved after practice.

At very low jet speeds ($M \approx 0{\cdot}3$), the wave intensity was so low as to merge with the background noise field. This set the lower limit on operational jet speed. By sophistication of the experimental environment the limit could have been lowered, but the associated decrease in Reynolds number to a substantially laminar régime would have soon set a final lower limit.

The data gathering equipment was of the analogue type which was not ideal for the particular low frequencies involved. A digital scheme would have had several advantages. The equipment used was, however, quite satisfactory for the the determination of the broad band intensity field.

The results obtained closely followed the theoretical prediction and brought out clearly the effect of turbulence at the nozzle exit as shown in figure 5 and table 2. The value of b^2 was found to be 0·3 which is comparable to the aerodynamic case (see, for instance, Voce & Lush 1969). For intense nozzle turbulence

a dipole field could be produced which was comparable to the radiation from the convected turbulence even at high subsonic Mach numbers.

It is concluded that this method of experimentation has much to offer in the quantitative study of various theoretical models and in the visualization of wave propagation.

Theoretical considerations

Ffowcs Williams & Hawkins obtained a two-dimensional result for shallow water wave generation by turbulence. The approach was essentially that used by Lighthill (1952) in his theory of aerodynamic noise. The major differences in the results obtained by Ffowcs Williams & Hawkins and those obtained by Lighthill arise through the change from three to two dimensions and not from the change of medium.

Shallow water wave propagation may be made virtually non-dispersive by choosing the correct water depth, namely 0·48 cm. At this depth the deviation of the wave speed c from $(gh_0)^{\frac{1}{2}}$ is of order $(kh_0)^4$ where k is the wave-number. This amounts to about 10 % for wavelengths of 1 cm, and less for longer waves. In this investigation no wavelength less than 1 cm was observed.

By considering the equations of motion and applying them to shallow water at the non-dispersive depth Ffowcs Williams & Hawkins obtained the non-homogeneous wave equation

$$\frac{\partial^2 h}{\partial t^2} - gh_0 \frac{\partial^2 h}{\partial x_\alpha^2} = \frac{\partial^2 T_{\alpha\beta}}{\partial x_\alpha \partial x_\beta},$$

where $T_{\alpha\beta}$ is the turbulence stress tensor, h the local water depth and α and β can take the values 1 and 2. They argue that $T_{\alpha\beta}$ is zero to second order in the perturbation field and is dominated by the term $hU_\alpha U_\beta$ where this is taken to be the average value of the Reynolds stress through the water depth.

The equation was solved in the same sense that the Lighthill–Curle (1955) equation represents a solution in the aerodynamic case. The general result revealed that the waves produced in the far field have a constant profile with an amplitude which goes as $r^{-\frac{1}{2}}F(t-r/c)$, r being the distance travelled and t the time. The field arises from a distribution of quadrupoles and surface dipoles, though in this case only quadrupole radiation is present due to the absence of solid boundaries.

The general theory was applied to the case of a free jet along which turbulence is convected. Dimensional analysis was then employed to obtain the parametric dependence of the far field mean square wave amplitude.

$$\overline{(h-h_0)^2} \sim (l/r_0)M^7[(1-M\cos\theta)^2+b^2M^2]^{-2},$$

l is the eddy length scale and r_0 the mean radiation distance.

In estimating this result certain assumptions are made. The turbulence length scales and the jet geometry are assumed independent of jet speed and the eddies to have a finite lifetime proportional to l/cM.

In practice the geometry remained fairly constant for all subsonic conditions; however, at higher speeds two effects were observed. The length of the jet increased with Mach numbers and at about Mach number 2 strong snaking occurred. The effect of the jet growth was not considered important at these supersonic conditions since the directionality of the radiation ensured that that which was measured came from the limited region of the jet which radiated most strongly. This is the first ten nozzle diameters or so. Further, the radiation at supersonic speeds originates from the single poles of the postulated quadrupoles and the near field effects diminish to render most of the environment effectively 'far field'.

The snaking, however, caused marked bunching in the radiated field due to changing radiation direction and Doppler shifts. Large-scale jet instability is likely to be the underlying cause of the snaking which may well be a yet unobserved feature of air.

Further details of a practical nature must be included in predicting the radiation field. The jet is obtained from a nozzle and certain aspects of this are important. On the inlet side of the nozzle there is a header reservoir tank into which water is run inevitably causing turbulence. This turbulence creates fluctuations in the mass flow rate through the nozzle, causing a monopole source term fixed at the nozzle exit. Ffowcs Williams (1969) has shown that the radiation goes as U^3 for this form of source.

Superimposed upon these fluctuations there is turbulence crossing the nozzle exit plane which in this particular case is largely generated by nozzle wall roughness. The turbulence creates at one point in the plane an outward fluctuation whilst at another point this is compensated by an inward fluctuation. This compensation must be complete at all times due to the near incompressibility of water. A dipole source is thus created. The length scale of this dipole, l_d, is set by the turbulence length scale which in turn is set by the nozzle width D. The frequency of radiation will go as cM/l_d, or cM/D, having an associated wavelength λ_d of cl_d/cM or D/M. In two dimensions the efficiency of such a dipole goes as $(\lambda_d/l_d)^2$ or M^2 (see Ffowcs Williams 1969). Thus the overall contribution to the radiation field from this source goes as U^3M^2. This, however, only applies to the subsonic case.

As the sonic speed is approached the radiation wavelength decreases until at the sonic speed it becomes similar to the dipole length scale. Under these conditions each pole operates independently as a monopole source so that as an approximation we may regard this the limiting case for dipole radiation. As radiation wavelength and jet speed are inversely proportional the restriction may be regarded as one of speed and the limiting condition becomes $M = 1$. Beyond $M = 1$ we have a U^3 dependence leading us to the final far field prediction for the radiation intensity given in (1) and (2). These equations are to be checked against experiment.

Experimental equipment

The basic equipment comprised a shallow water table, a Perspex nozzle (figures 1 and 2, plate 1) and a capacitance proximity gauze. The bottom of the table was a glass plate measuring 2·44 by 4·88 metres. This was supported by a matrix of 2·5 cm pads placed in square form 30·5 cm apart. These pads were adjusted so as to make the glass level and flat to a local gradient of $\pm 2{\cdot}5 \times 10^{-4}$, thus ensuring a good eveness of water depth. The whole of the glass plate was surrounded by a stainless steel tray. Ripple absorbent, animal wool beaches were placed in the steel tray.

The water depth could be initially set using a spherometer to $\pm 0{\cdot}01$ cm, then maintained to within 0·002 cm throughout the gathering of any particular series of data points. A capacitance proximity gauze was mounted on a movable gantry spanning the width of the water table.

The nozzle had a header reservoir tank 35 cm high to supply the motive force for the jet. The nozzle itself was 'stopped down' to the nominal water depth h_0 (0·48 cm). The correct expansion for the jet was thus obtained, in a sense, automatically, enabling the single nozzle to be used for all jet speeds. The nozzle exit cross-section was $0{\cdot}48 \times 2{\cdot}5$ cm. The jet speed was obtained by measuring the mass flow rate into the header tank. Leakage between the nozzle and water table was prevented by the use of grease and weights. Wall roughness was provided by brass shims fixed to the inside of the nozzle (figure 2, plate 1), these could be altered.

A capacitance proximity gauge was used for wave monitoring since it had a negligible interaction with the wave field. The particular device used was made by Wayne Kerr: their vibration meter B 731B and probe MC1. The range of the probe was about 0·025 cm, and had an effective diameter of a little over 0·5 cm. The electronics line-up is shown in figure 3. The squarer was derived from the Fenlow Analogue Multiplier Type MX 101. The averaging circuit had a time constant of about 100 sec.

The system was calibrated in two stages, a static calibration of the probe and the B 731B, and an electronic calibration of the rest of the system in the range of frequencies of interest (0·1 to 30 Hz).

The static calibration was achieved for incremental changes in distance by accurately monitoring the output of the B 731B (using a digital voltmeter) for calculated changes in water depth. The latter was obtained by making small measured additions of water to the water table and calculating the change in depth, subtracting the amount lost to evaporation during the 'settling period'. The 'settling period' was the time it took to achieve a near ripple free surface after the addition of water (typically 1 to 2 min.). As the evaporation was equivalent to a voltage drift it was this which was estimated and added to the voltage change at the B 731B output. The rate of voltage drift due to evaporation was found to be typically 1 mV per min. This is approximately equivalent to an evaporation rate of 2×10^{-5} cm per min.

It was also found that the dynamic response of the Wayne Kerr equipment

looked extremely good on visual monitoring up to 25 Hz, the highest frequency at which the probe was vibrated above the water.

The back-up electronics was tested for the particular output voltage changes and signal frequencies that would be expected from the filter after the B 731 B. It was found that the squarer squared accurately and that the overall gain of the system was independent of frequency in the relevant range. Care had to be taken, however, to stay within the working amplitude range of the squarer. This was achieved by having a variable gain preamplifier before the squarer.

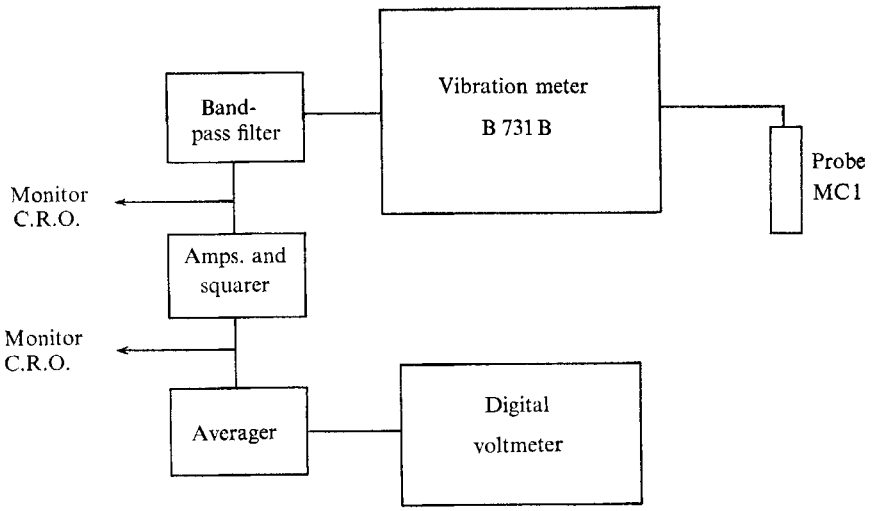

FIGURE 3. Schema of electronics.

By combining the calibration measurements, an overall calibration was obtained and found to be linear as depicted in figure 4. In this investigation the linearity was the important feature since a decibel scale based on an arbitrary datum would be used for intensities.

In fact, the wave intensities varied over some 60dB which was greater than the transducer range. This was overcome by using three observation positions which were as in table 1. The jet direction is taken as Y and the orthogonal direction in the plane of the table as X.

Position	Y (cm)	X (cm)
(i)	56	53
(ii)	112	91
(iii)	142	107

TABLE 1

The use of the various positions was dependent on the intensity of the radiation. The greater distances were used for the higher intensities, i.e. with the higher speeds. A reasonable velocity overlap was made between positional moves in order that the series of data points obtained at each position could be blended

into one curve. This meant multiplying the intensities obtained at positions (ii) and (iii) by a suitable factor in each case.

Due to the fairly low Reynolds numbers involved at low speeds some turbulence had to be given to the jet to initiate the jet instability. The turbulence was then maintained by the flow as assumed by the theory. The initial turbulence was in all cases derived from nozzle wall roughness.

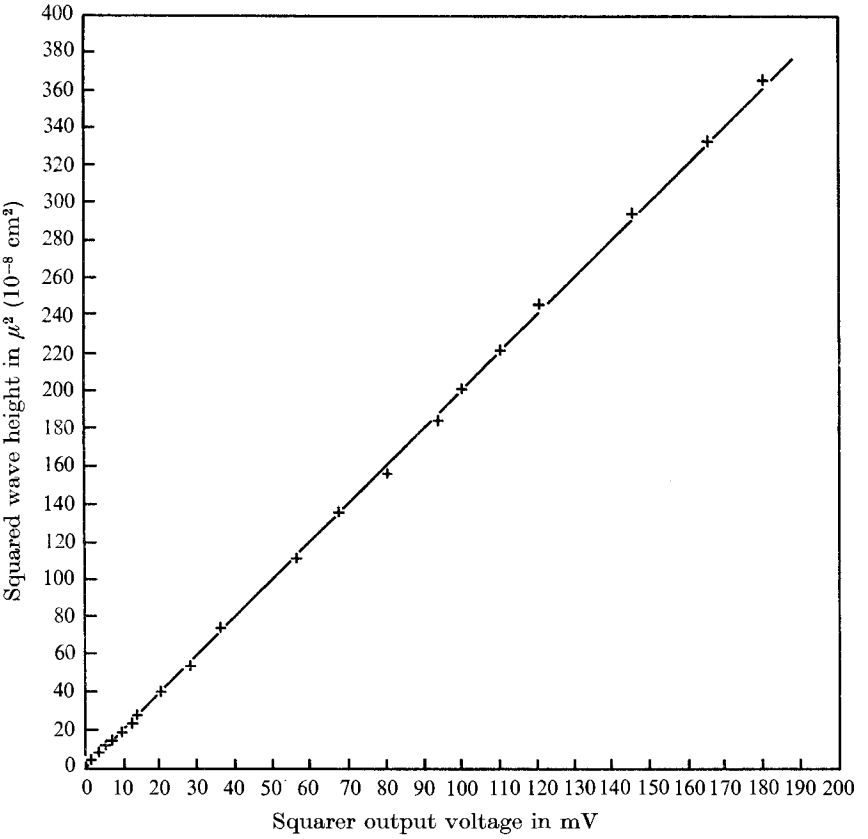

FIGURE 4. Calibration curve.

The investigation

As a preliminary to the main part of the investigation, propagation from a simple source (a harmonic plunger) was examined. It was found that the ripple intensity fell off at a rate greater than r^{-1}; this was due to attenuation. If the attenuation over one typical eddy dimension was significant, the radiation from the associated quadrupole radiator would be enhanced by a reduction of the destructive interference between source elements. An investigation of attenuation was therefore undertaken.

It was found, as might have been expected, that the attenuation coefficient depended to a great extent on the cleanliness of the water surface. After an exposure to the prevailing laboratory atmosphere for about five hours the

attenuation was about 1 dB per nozzle diameter. After exposure for less than about one hour the attenuation was only 0·3 dB per nozzle diameter. It was further found that the attenuation depended on wave-number.

It was apparent that for very fresh water (i.e. clean), the attenuation was very low indeed. It was not clear how the attenuation could be measured under these conditions. The complicating factor was the length of experimental time required, about 25 min, during which the water became contaminated. The jet would, in fact, be working under such clean conditions, since the influx of fresh water from the nozzle and the surface skimming effect of the table outlet ensured a constant renewal of water surface.

It was decided that the investigation would be carried through and the attenuation neglected.

The set-up has partially been described already. The water depth was set at 0·48 cm. The capacitance probe was mounted on the gantry such that the face of the probe was some 0·02 cm from the water surface and its face as near parallel as could be achieved by eye. The table outlet and jet speed were so adjusted as to give a water depth which was steady to at least 2×10^{-4} cm per min. If the water depth drifted quicker than this an artificially high reading would be obtained. Much time was spent in adjusting the table outlet. After some practice one data point could be gathered every 20 min or so. One other difficulty was air movement above the water and mechanical vibration through the table structure, probe mount and gantry. This was especially important at very low wave intensities. The air movement was minimized by the exclusion of drafts and all movement in the laboratory. A measurement of the background wave intensity and vibration was made with no jet flow and this was subtracted from the readings obtained. This was not very satisfactory, however, since the background measurement varied considerably over times similar to those taken in making measurements.

The jet measurements were carried through for three degrees of wall roughness. A comprehensive jet speed range was used for the case of moderate roughness. This involved moving the observation point to all three positions mentioned earlier. For the other two roughnesses, one of less roughness and one of greater roughness, only a limited speed range was used and all measurements were made at position (i).

Results

From photographic evidence (see figure 6, plates 2 and 3), the eddy Mach number was estimated at 0·6 of the jet Mach number. The angle θ was taken to be approximately 45° and the best fitting curve was found by varying b, A and B. The value of b which gave the best normalization of the data was 0·55 ($b^2 = 0{\cdot}3$). The values of A and B depended on the wall roughness used in each case. This can be seen in table 2 and figure 5. The value of A was indeed independent of B, but B was greatly dependent on the degree of roughness.

Photographic evidence revealed that increased roughness also led to increased forward throw.

Roughness (ascending) order	A	B	Symbol used in figure 5
1	0·15	0·3	△
2	0·15	2·0	○
3	0·15	5·0	+

TABLE 2

The dependence of the radiation field at high speed would be expected to go off asymptotically as the cube power of the Mach number. However, for the particular value of the eddy life parameter found here, this dependence comes at Mach numbers in excess of those investigated. This is unlike the aerodynamic case where the variation in power law is far more damped, for a similar value of b^2.

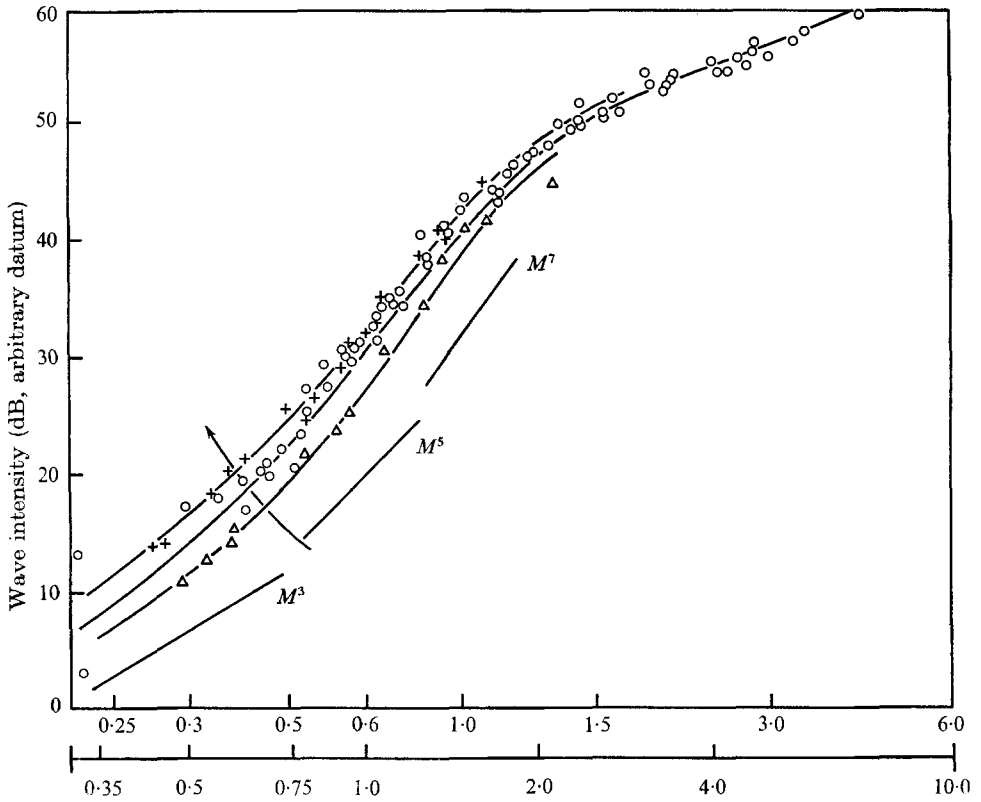

The arrow indicates increasing nozzle roughness.

FIGURE 5. Radiation *vs.* Mach number.

Discussion

The main conclusion to be drawn from this investigation is that this method of simulation shows great potential for future investigations. The theoretical model used for the jet is obviously an extremely good one and since it was derived from a more general result (Ffowcs Williams & Hawkins 1968, equation (3.7)) it may be expected that equally good results may be obtained in other problem studies. Scope for future work is obviously very wide.

Some ideas of a practical nature to improve data gathering are the possible digitalization of an analogue signal and computerization, better isolation of the experimental environment, and possible dust screening where the flux of water through the table is near zero. A further point can be made on the use of capacitance probes, the probe used had a circular plate and was thus omni-directional. It is possible to give the probe used some directional characteristics by re-designing the probe plate. A long rectangular one would, for instance, receive preferentially (especially for short wavelengths) in the direction normal to the longer side.

The author is grateful for the supervision of Dr J. E. Ffowcs Williams and Dr J. K. Harvey. The work was sponsored by the Ministry of Technology.

REFERENCES

CURLE, N. 1955 The influence of solid boundaries upon aerodynamic sound. *Proc. Roy. Soc.* A **231**, 505–514.

FFOWCS WILLIAMS, J. E. 1969 Hydrodynamic noise. *A.R. Fluid Mechanics* 85378, p. 579.

FFOWCS WILLIAMS, J. E. & HAWKINS, D. C. 1968 Shallow water wave generation by unsteady flow. *J. Fluid Mech.* **31**, 779–788.

LIGHTHILL, M. J. 1952 On sound generated aerodynamically. I. General theory. *Proc. Roy. Soc.* A **211**, 564–587.

VOCE, J. D. & LUSH, P. A. 1969 An application of quadrupole theory to correlate the directivity and spectra of high speed jet noise. *AGARD PREPRINT* no. 42.

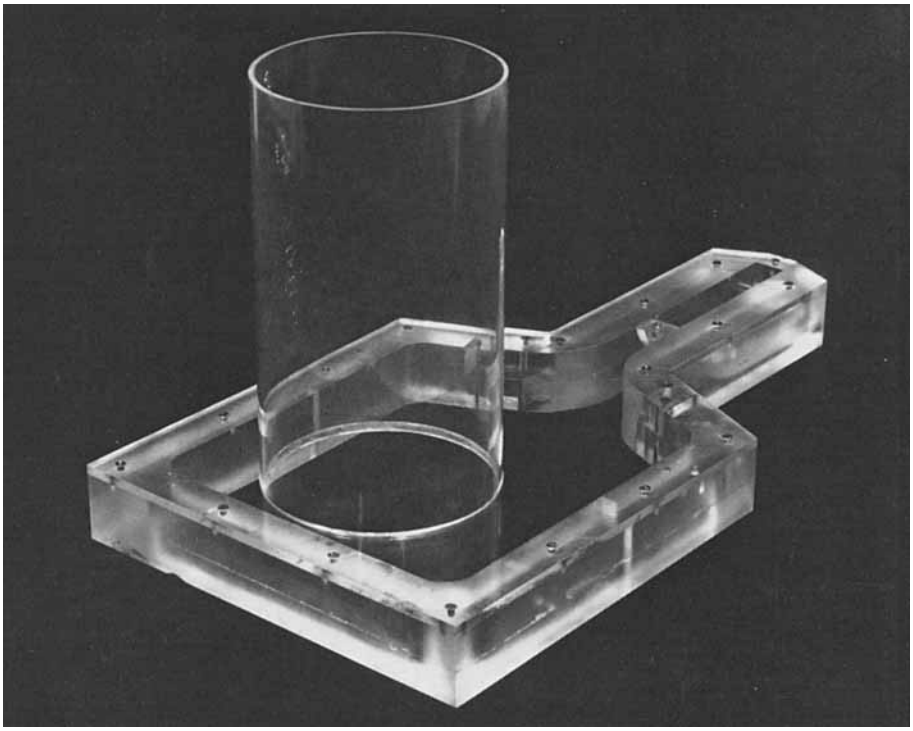

FIGURE 1. Nozzle and header tank.

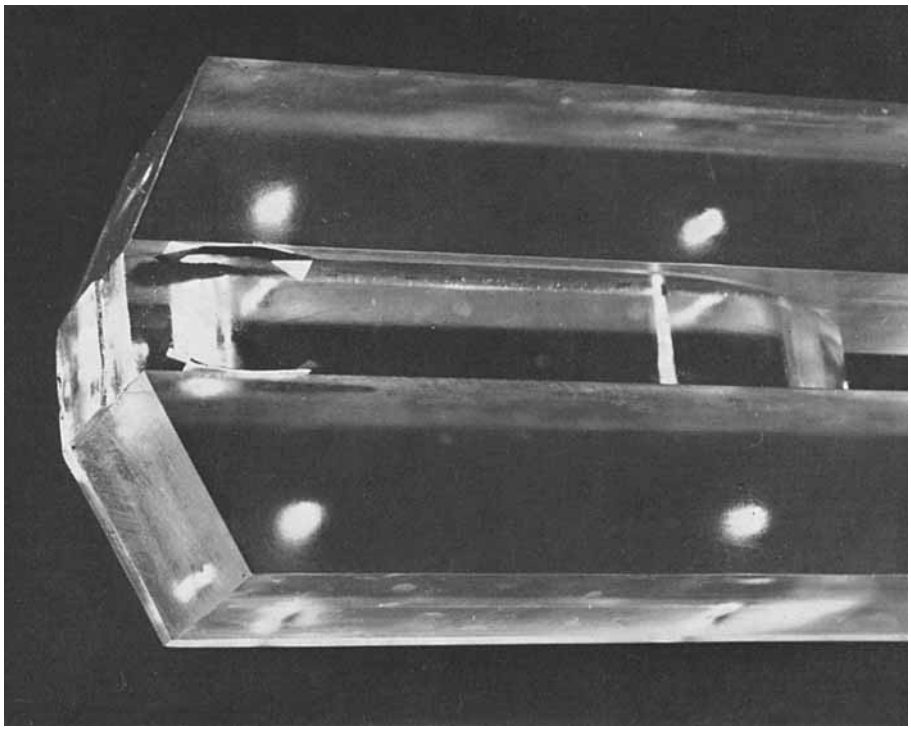

FIGURE 2. Nozzle showing roughness.

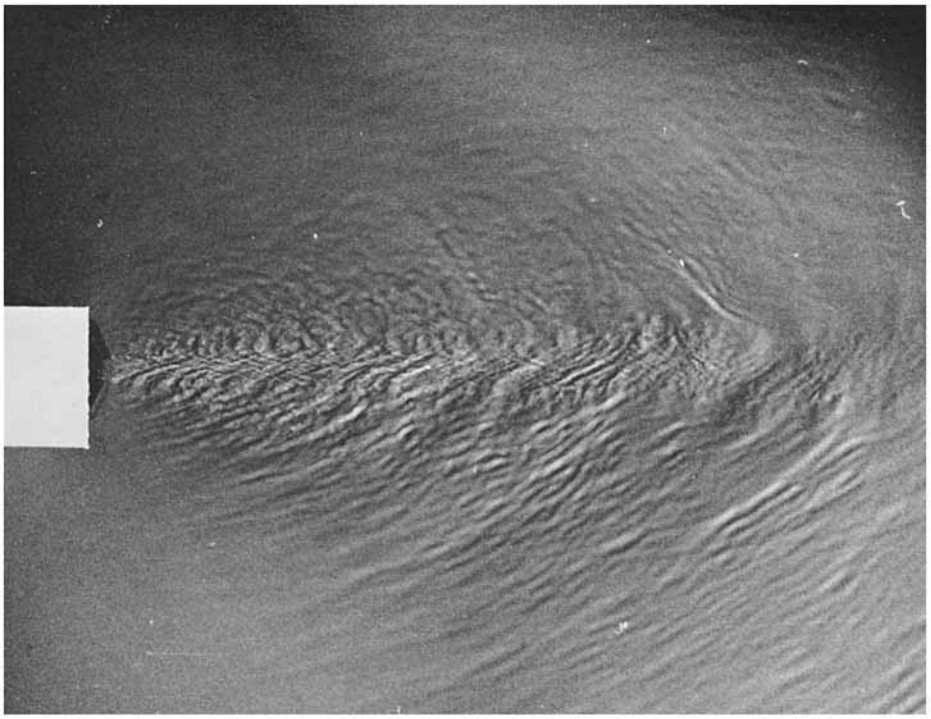

(*a*)

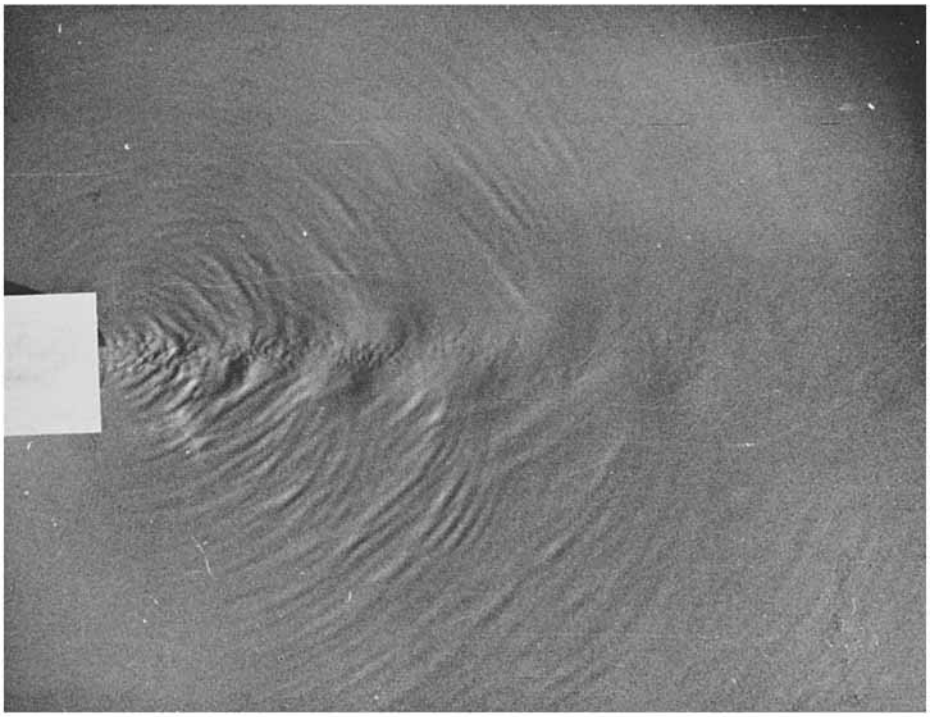

(*b*)

For legend see plate **3.**

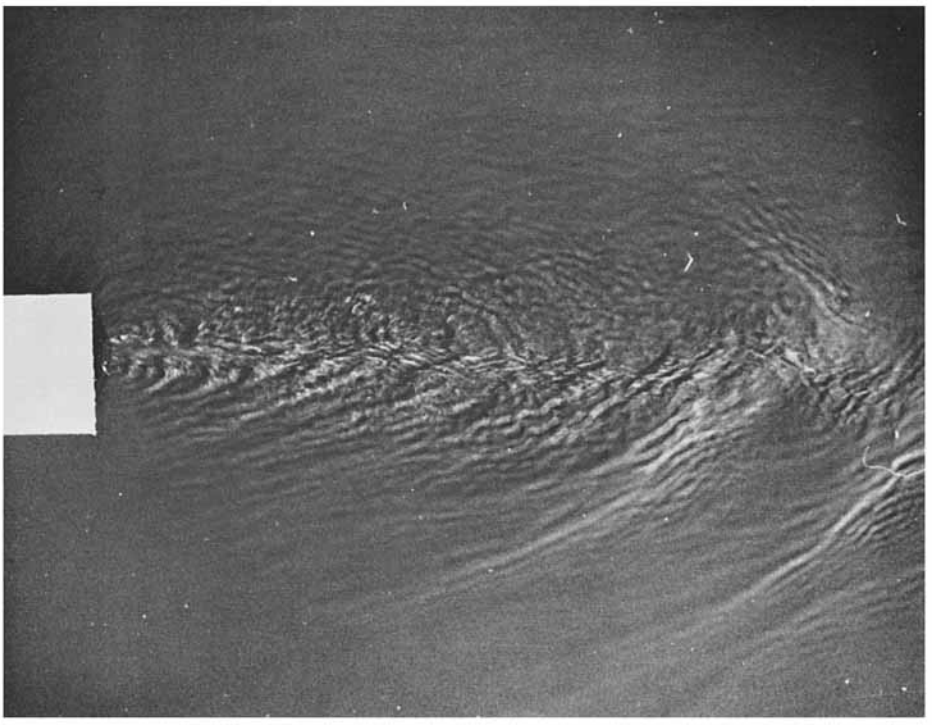

(*c*)

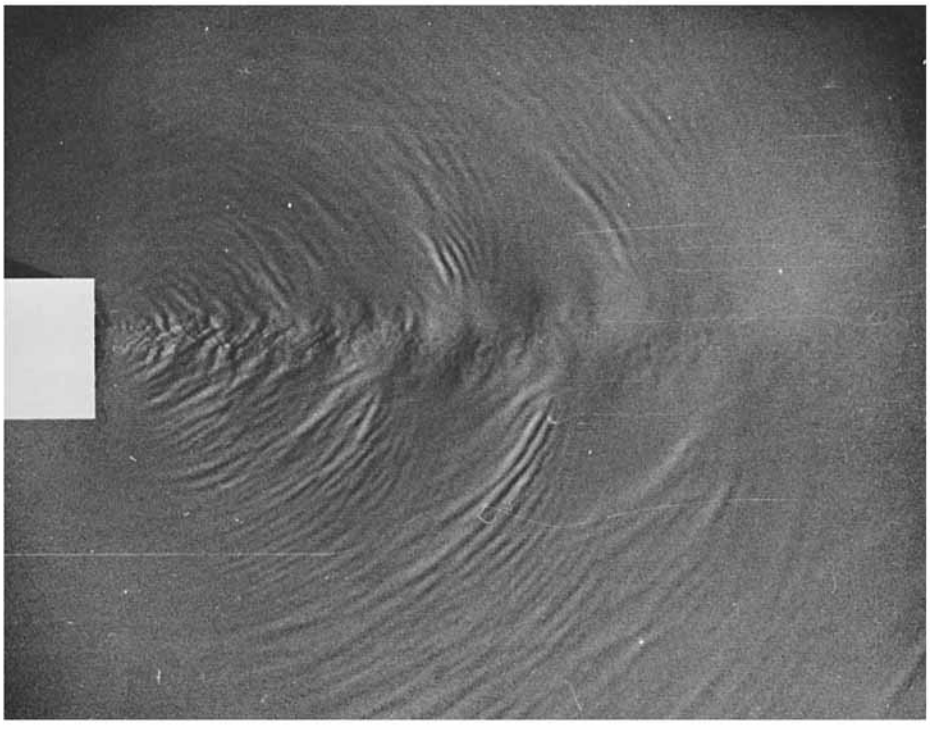

(*d*)

FIGURE 6. Various jets. (*a*) Smooth nozzle, jet Mach number = 5. (*b*) Smooth nozzle, jet Mach number = 2·5. (*c*) Rough nozzle, jet Mach number = 6. (*d*) Rough nozzle, jet Mach number = 2.